Proceedings of the ASME 2018
5th Joint US-European Fluids Engineering Division Summer Meeting
FEDSM2018
July 15-20, 2018, Montreal, Quebec, Canada

FEDSM2018-83300

INFLUENCE OF TYPICAL SUBGRADE STRUCTURES ON AERODYNAMIC CHARACTERISTICS OF HIGH SPEED TRAINS IN CROSS WIND CONDITIONS

Zhenxu SUN
Key Laboratory for Mechanics in Fluid Solid Coupling Systems, Institute of Mechanics, Chinese Academy of Sciences
Beijing, China

Guowei YANG
Key Laboratory for Mechanics in Fluid Solid Coupling Systems, Institute of Mechanics, Chinese Academy of Sciences
Beijing, China

ABSTRACT

Due to geographical and environmental constraints, high-speed railways use a variety of subgrade structures such as ground, embankments with different height, viaducts, etc. When trains run on embankments and viaducts, the flow around the car body is more complex than the ground. Under the action of crosswind, there are obvious differences in the cross-wind aerodynamic characteristics of high-speed trains on different subgrade structures. The unreasonable subgrade structure will affect the cross-wind safety of the train. At the same time, the structure of the train is complex, the bogie and pantograph have an important role on the flow field characteristics of the train, and the over simplified profile of the short train cannot accurately reflect the true aerodynamic characteristics of the train. In the present paper, in order to study the influence of typical subgrade structure on the aerodynamic characteristics of high speed trains, a real high-speed train with 9 carriages at the speed of 200 km/h was taken for case study, and the details of windshields, bogies and pantographs were taken into consideration. The cross wind velocities were chosen as 20, 30, 35 and 40 m/s. The aerodynamics performance of the high-speed train under the four conditions of plane ground, 3m-embankment, 6m-embankment and viaduct were simulated and compared, and the differences and regularities in the aerodynamic characteristics under cross wind conditions on different subgrade were analyzed. The results provide a reference for train safety control on complex subgrade structures under cross wind condition.

1 INTRODUCTION

When running in conditions with strong cross wind, the aerodynamic performance of high speed trains (HSTs) will deteriorate dramatically, including the running stability and the increasing risk of derailment [1]. For some subgrade structures such as embankments with different heights, viaduct et al, different flow patterns around the train will be induced compared to the ground circumstance. Meanwhile, the lateral force and overturning moment of the train are also increased. Derailment will happen when the cross wind speed exceeds the critical overturning wind speed, which would greatly affect the running safety of HSTs. Over the past few decades many studies have been performed on aerodynamic performance of HSTs in cross wind conditions: Suzuki [4] experimentally studied the influence of different bridge structures and embankments on flow field near the train in the wind tunnel, and found the difference of the flow field under different yaw angles of the incoming flow and different train shapes. Diedrichs [5] performed the study of running stability of HSTs on the embankment in cross wind conditions. Bocciolone [6] experimentally studied the aerodynamic performance for HSTs with three different shapes under different incoming flow conditions and different subgrade conditions. Xi YH [7] studied the aerodynamic performance of HSTs under different running speeds and different crosswind speeds, and obtained the relationship between the maximum running speed and cross wind speed in cross wind conditions. Li T [8] studied the aerodynamic performance for HSTs passing by the wind-break walls with different heights, and then proposed the way to improve the design of wind-break walls. Based on theories of

aerodynamics and multi-body dynamics, Zhang L [9-10] analyzed the time-domain and frequency-domain characteristics of unsteady loads on train body and pantograph in cross wind conditions. On the base of vehicle dynamic coefficients, track irregularity characteristics and instantaneous maximum wind speed, Miao BR [11] built a multi-body dynamic model for the whole train and investigated on the running safety problem under unsteady aerodynamic loads. He XH studied the influence of wind-break walls on pressure distribution and aerodynamic loads distribution on HSTs for HSTs running on a typical viaduct in cross wind conditions. Luo JB [13] studied the influence of obliquity of the embankment on aerodynamic characteristics of HSTs in cross wind conditions.

Most of current studies focus on different train shapes and different cross wind speeds. However, there are few studies to be referred to for the influence of subgrade structures in cross wind conditions, especially the systematical study of flow structures in cross wind conditions under different subgrade structures, no matter the studies in domestic or abroad. Based on the study of above literatures, the influence of subgrade structures on aerodynamic performance of HSTs in cross wind conditions has been systematically studied in the present work, and four typical subgrade structures are considered, including the ground, 3m-height embankment, 6m-height embankment and viaduct.

2 COMPUTATIONAL MODEL AND ALGORITHMS

2.1 COMPUTATIONAL MODEL

Complex detached vortices in the leeward side will rise when HSTs run in cross wind conditions. How to simplify the computational model will greatly affect the vortex structures. In order to avoid this problem, a real train model has been adopted for the computational train model, which includes a power leading car, seven middle carriages and a trailing car. Meanwhile, the windshields, bogies and pantographs are all considered in this real train model. The computational train model are shown in Figure 1. As shown in Figure 1, the total length of the train is about 228m, and the height of the train is 3.8m. The pantographs are installed on the leading car, which are shown in Figure 2.

Figure 1. Computational train model.

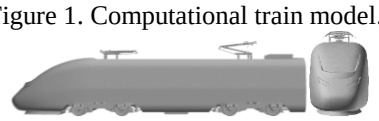

Figure 2. Computational model of the leading car.

2.2 SUBGRADE STRUCTURES

The running circumstance varies drastically for high speed trains, and the subgrade structures usually have different forms. Some typical subgrade structures are usually faced, which are ground, embankment with different heights, and viaducts. In the present paper, the ground, 3m-height embankment, 6m-height embankment and viaduct are chosen as the basic subgrade structures, which are shown in Figure 3. These four subgrade structures could basically contain the frequently-met cases, and the study on these subgrade structures could shed lights on the influence of subgrade structures on aerodynamic performance of HSTs in cross wind conditions.

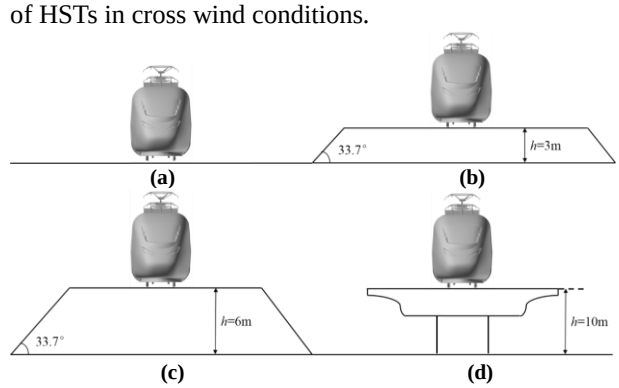

Figure 2. Different subgrade structures: (a) Ground; (b) 3m-height embankment; (c) 6m-height embankment; (d) Viaduct.

2.3 COMPUTATIONAL ALGORITHMS

The running speed of the train is 200 km/h, and the Mach number is less than 0.3. As a result, the three-dimensional unsteady incompressible Reynolds Averaged Navier-Stokes (RANS) equations are chosen as the governing equations. Considering the unsteadiness in specific locations of the flow field, the k-w SST model is adopted for turbulence enclosure. It is a kind of hybrid model which turns to the Wilcox k-w model in near-wall zones while turns to the k-epsilon model outside the boundary layers. A hybrid function is utilized for the transition of models. Essentially, it belongs to a two-equation eddy viscosity model with its transport variables integrating to the walls for incompressible/compressible flows [14].

3 COMPUTATIONAL CONDITIONS AND MESH DISTRIBUTION

3.1 COMPUTATIONAL CONDITIONS

The finite volume method based on cells is adopted for the discritization of the controlling equations. A second order upwind scheme is used for convection terms while for viscous terms the second order central differentiation scheme is used. A completely implicit scheme is adopted for time discritization. Meanwhile, the standard wall function is used for near wall treatment. Considering the high speed train runs at a subsonic speed, the Riemann invariant is adopted to solve the variables at far field boundaries. As a result, the inlet, outlet and far field of the computational domain are all set as non-reflective boundary conditions. A no-slip wall condition is used for the train surface. In order to simulate the ground effect caused by the relative motion between the train and the ground, a moving wall

boundary with the same speed of the inlet boundary is adopted for the ground.

3.2 COMPUTATIONAL DOMAIN AND MESH DISTRIBUTION

Taking H as the height of the high speed train, the upstream length is set as 30H while the downstream length of the domain is set as 60H. The width and height of the domain are set as 30H, just as Figure 4 shows.

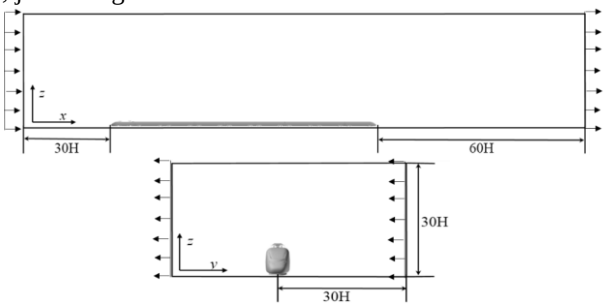

Figure 4. Computational domain.

The trimmed mesh has been utilized in present work and the prism layers are also adopted in the near wall zone. The value of y+ in the first prism layer varies from 30 to 120 to ensure the use of wall functions. In order to precisely capture the trail vortices, the wake zone has been densified where the smallest length scale is around 6cm. The total amount of the mesh is 52 million. Representative mesh of different locations is shown in Figure 5 and Figure 6.

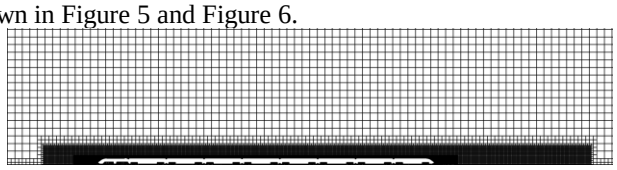

Figure 5. Mesh distribution in the longitudinal section.

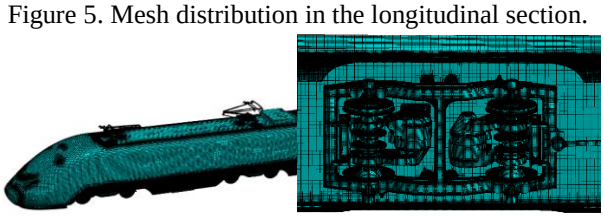

Figure 6. Representative mesh of different locations.

3.3 CASES SUMMATION

The generation and evolution of vortices in the leeward side and the wake zone are seriously affected by the subgrade structures and cross wind conditions. In the present work, four subgrade structures and four cross wind conditions are considered, which are listed in Table 1.

Table 1. Cases summation

Subgrade Structures	Cross wind speed(m/s)
Ground	20
3m-height embankment	30
6m-height embankment	35
viaduct	40

The running speed of the train is 200 km/h. For each subgrade structure, all four cross wind speeds are considered. Consequently, the total number of cases is 16.

4 RESULTS AND DISCUSSIONS

4.1 SURFACE AND SPATIAL DISTRIBUTION OF PRESSURE

The flow structures around the train are the root to aerodynamic performance of HSTs. In cross wind conditions, aerodynamic performance will deteriorate drastically. Compared to the ground, other subgrade structures such as embankment and viaduct will alter the flow structures around the train dramatically and consequently affect the aerodynamic performance. The pressure distribution along the train plays an important role for aerodynamic loads, and influence directly on each carriage's aerodynamic forces. Taking the cross wind speed of 20 m/s as an example, Figure 7 and Figure 8 show the pressure distribution on the leading and trailing cars under different subgrade structures.

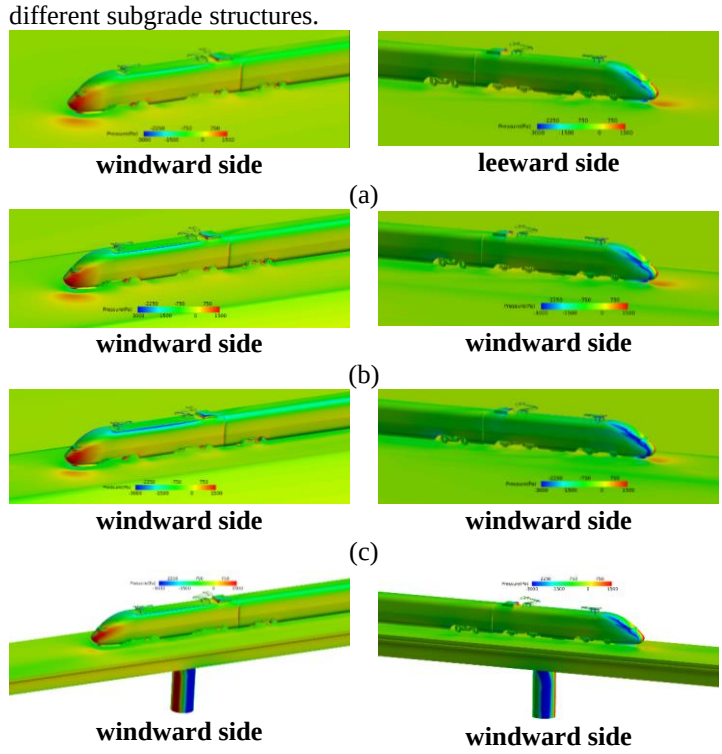

Figure 7. Pressure contour of the leading streamline: (a) Ground; (b) 3m-height embankment; (c) 6m-height embankment; (d) Viaduct.

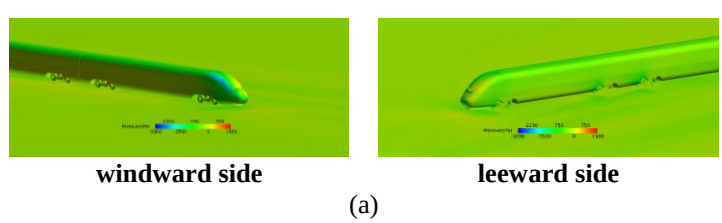

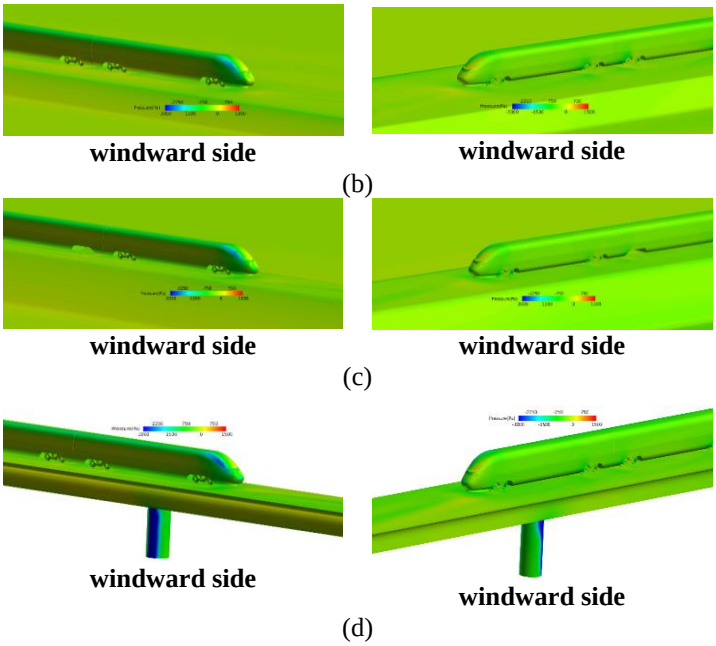

Figure 8. Pressure contour of the trailing streamline: (a) Ground; (b) 3m-height embankment; (c) 6m-height embankment; (d) Viaduct.

Strong asymmetry could be observed for the pressure distribution on the train body due to the cross wind effect. As Figure 7 shows, the stagnation zone in front of the leading nose shifts to the windward side. High pressure could be found in the windward side of the pantograph and the bogies. However, due to the existence of massive vortices in the leeward side of the train, big low pressure zone could be found along the leeward side surface. In the cross wind condition, the upwind area of the train increases and much more air flows into the gap between the bottom of the train and the rail, resulting in higher resistance on the bottom structures. The pressure on the windward side of trailing nose is negative while that is near 0Pa on the leeward side. The pressure on the cab window of the trailing nose is positive with a relatively small value.

Strong ground effect exists when HSTs run and influence between the ground and train is very obvious. The ground which is just beneath the trailing nose also owns high positive pressure. The nearer to the leading nose, the higher the pressure on the ground is. However, the difference of subgrade structures could lead to the difference of pressure distribution on the ground. On the condition of the same running speed and the same cross wind speed, the area of high pressure zone on the ground for the viaduct case and the 6m-height embankment case is obviously smaller than the ground case and the 3m-height embankment case. For the ground case, the cross wind blows directly on the leading nose. However, for the embankment structures, the cross wind blows on the bottom of embankment in advance and then flows along the side of the embankment, generating a recirculation zone on the top of the embankment. As a result, the impingement on the train body is weakened. For the viaduct case, the cross wind could flow both up and beneath the viaduct, and the recirculation zone on the windward side could also weaken the impact on the leading nose. Based on the above analysis, it could be deduced that the drag on the leading car for the viaduct and 6m-height embankment cases will be smaller than that for the ground and 3m-height embankment cases. It could also be found that the absolute value of negative pressure on the leeward side of the leading car for the viaduct and 6m-height embankment cases is bigger than that for the ground and 3m-embankment case. This is due to the fact that the vertical velocity gets increased due to the induction of the windward side of subgrade structures. The negative pressure on the trailing nose for the viaduct case is much stronger that the other three cases. The cross wind could flow beneath the viaduct, which could strengthen the leeward vortices.

The space distribution of the pressure and velocity could do damage to the surrounding buildings and workers [15]. Figure 9 and Figure 10 show the pressure contour on z=0.2m and z=1.4m plane when the cross wind speed is 20 m/s. From the view of flow structures, these two heights corresponds to the smaller vortices emerging from the bogie zone and the bigger vortices emerging from the train body. From the view of safety, these two heights correspond to the height of baggage and passenger. As a result, it is very crucial to obtain the pressure distribution on these two heights. It could be seen that the negative pressure zone in the leeward side for the 6m-height embankment is quite larger that the case of ground and 3m-height. Among all four subgrade structures, the negative pressure in the wake zone for the viaduct case is the strongest. It is the same with the analysis of leading nose, the cross wind is firstly blocked by the bottom of embankment and then get risen along the embankment side. As a result, small vortex structures generate at the bottom of the embankment and strengthen the evolvement of the vortices in the leeward side. Consequently, the negative pressure in the leeward side gets strengthened.

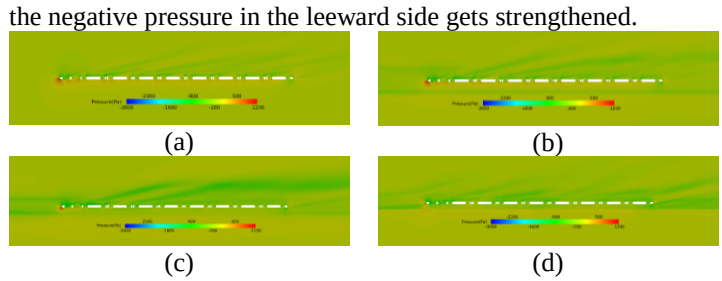

Figure 9. Pressure contour at z=0.2m for different subgrade structures: (a) Ground; (b) 3m-height embankment; (c) 6m-height embankment; (d) Viaduct.

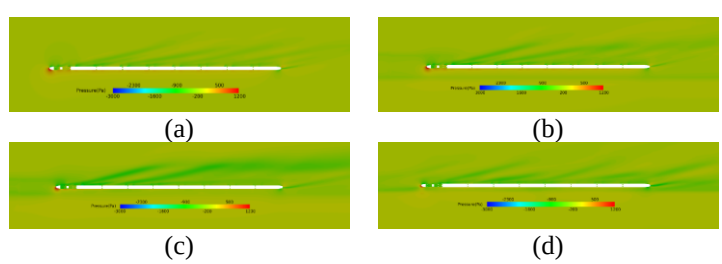

Figure 10. Pressure contour at z=1.4m for different subgrade structures: (a) Ground; (b) 3m-height embankment; (c) 6m-height embankment; (d) Viaduct.

4.2 VORTEX STRUCTURES IN THE LEEWARD SIDE

In the cross wind conditions, the intensity and numbers of vortices in the leeward side of the train would influence greatly on the aerodynamic performance, running stability and aerodynamic noise. As a result, it needs to be deeply studied. Five cross-sections have been selected along the train to be studied, as shown in Figure 11.

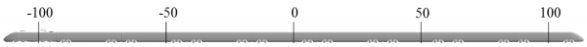

Figure 11. Locations of five cross-sections.

Taking the cross wind speed of 20 m/s as an example, the distribution of velocity vector on the five sections are shown in Figure 12, which could represent the evolvement of leeward vortex structures from the leading car to the trailing car. For the four subgrade structures, some common phenomena could be observed: at x=-100m, the vortex V1 is very close to the train body. While at x=-50m, V1 is shifted outward and get bigger. Meanwhile, a new vortex V2 has developed at a relative long distance from the train body. For the sections of x=50m and x=100m, the vertices get stronger and stronger when they evolve downstream, and the influenced area gets increased as well. For the case of 6m-height embankment and viaduct, the vortex structures exist not only in the leeward side, but also on top of the subgrade in the windward side, which is named as V3. V3 is a result of rough change of the shape.

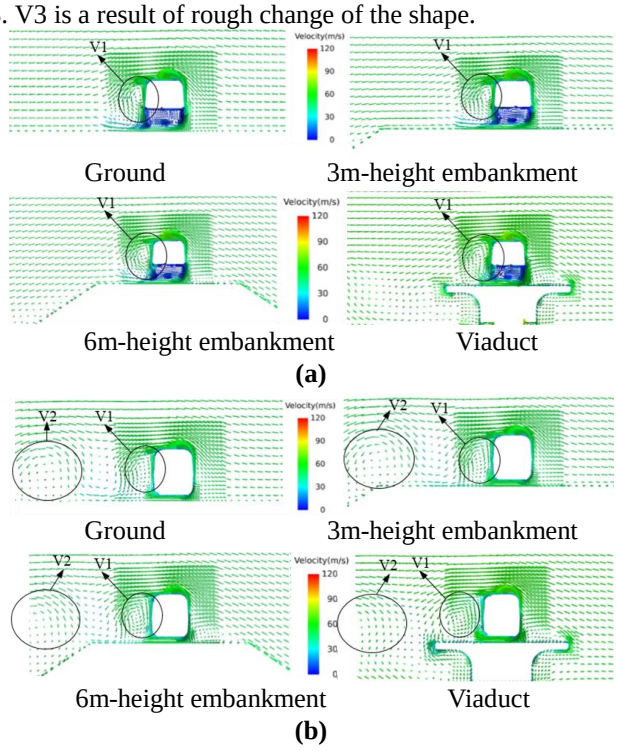

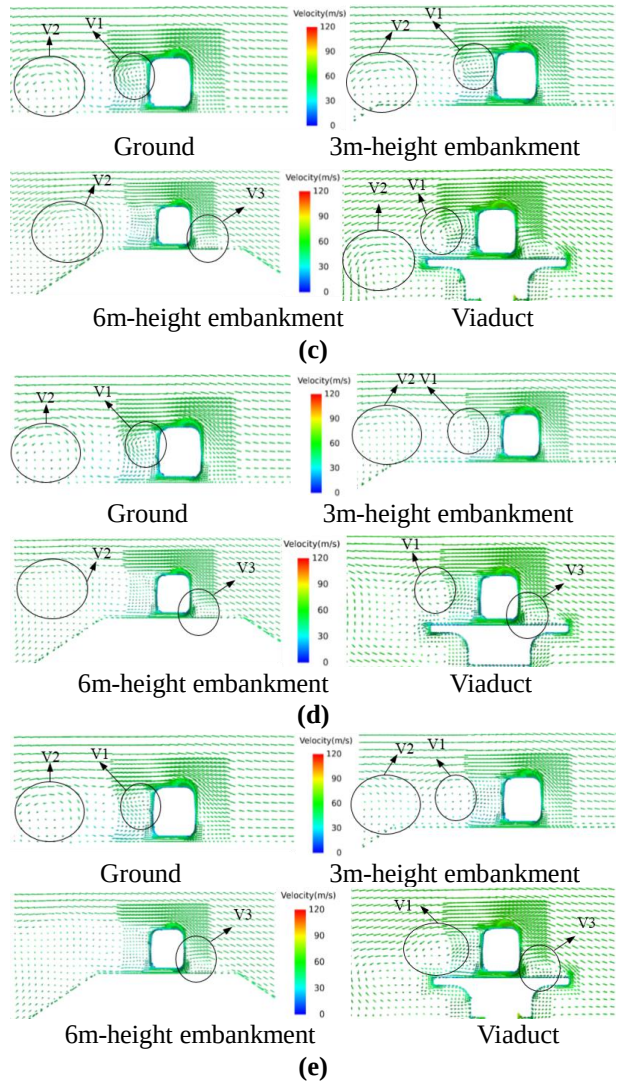

Figure 12. Distribution of velocity vector on the five sections: (a)x=-100m; (b)x=-50m; (c)x=0m; (d)x=50m; (e)x=100m.

4.3 VORTEX STRUCTURES IN THE WAKE ZONE

The trailing vortices and their evolvement affect greatly on the lift of the trailing car and running stability of the train. Figure 13 shows the iso-surface of Q for different subgrade structures. Q is defined as the second invariant of velocity tensor and could be used to represent the local vortex structure. As shown in Figure 13, one main vortex could be found in the wake zone. It detaches from the side of the cab window on the trailing car. The surface separation line could be obtained by surface streamlines, which also indicates that the trailing vortex detaches from the windward shoulder of the trailing streamline. Meanwhile, smaller vortices at the bottom and leeward side of the trailing car could be observed. These smaller vortices are mainly induced by the bogies and windshields. For the viaduct case, more vortices could be found at the side of the viaduct and the pillars. These vortices could gradually influence the upper

vortices along the train body, and consequently, affect the aerodynamic performance. Figure 14 shows the surface streamlines on the trailing car. It could be seen that the separation line for the ground case and 3m-height embankment case are close to the cab window while that for the 6m-height embankment case and the viaduct case are beneath the cab window.

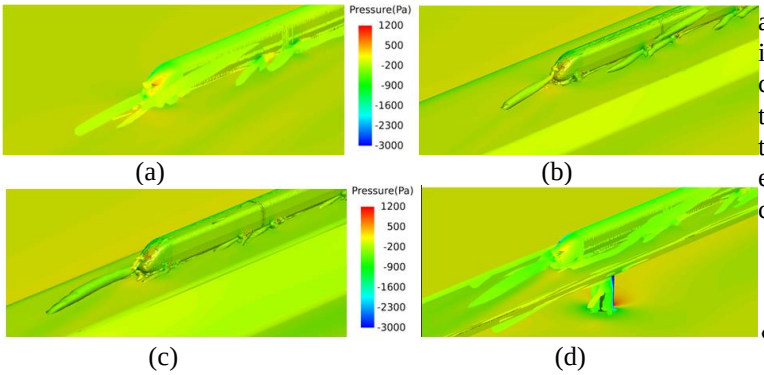

Figure 13. Iso-surface of Q (Q=100)for different subgrade structures: (a) Ground; (b) 3m-height embankment; (c) 6m-height embankment; (d) Viaduct.

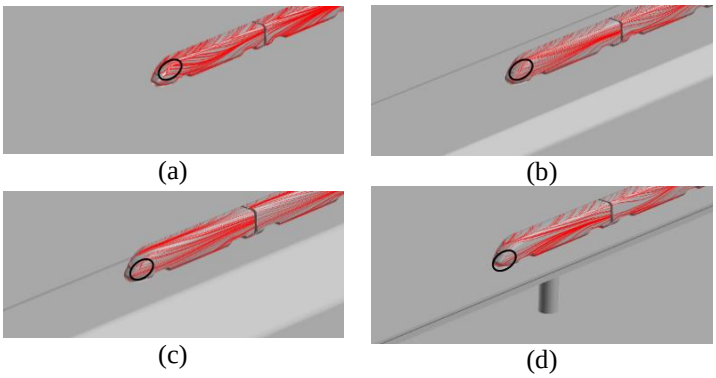

Figure 14. Surface streamlines on the trailing car: (a) Ground; (b) 3m-height embankment; (c) 6m-height embankment; (d) Viaduct.

4.4 AERODYNAMIC LOADS

Aerodynamic performance for HSTs in cross wind conditions could be affected not only by the speed of cross wind, but also by the subgrade structures. In the present work, four cross wind speeds have been considered for all the four subgrade structures, and aerodynamic loads for each carriage have been carefully compared.

Figure 15 shows the comparison of aerodynamic drag of each carriage with different cross wind speeds. It can be seen that, in ground condition, aerodynamic drag increases with the cross wind speed. However, the drag of the leading car decreases with the cross wind speed for most cases. For the 6m-height embankment case and viaduct case, the drag of the leading car becomes negative as the cross wind speed goes up to a certain value. As the running speed keeps constant, the bigger the cross wind is, the larger negative pressure zone on the leading streamline, which could generate thrust on the leading car. For the cross wind speed of 20 m/s, the drag of the leading car is the biggest for the ground case, while it is the smallest for the viaduct case, which is consistent with the former flow field analysis. For all cases, the drag of the trailing car increases with the cross wind speed. For the ground case and embankment cases, the drag of the middle carriage keeps almost the same. However, it varies a lot for the viaduct case, indicating that the distribution of aerodynamic loads on each carriage is much more uneven when HSTs run on viaduct. Since there is big space beneath the viaduct, the interaction between the upper and lower flow is much stronger, which could exaggerate the difference of aerodynamic loads on each carriage.

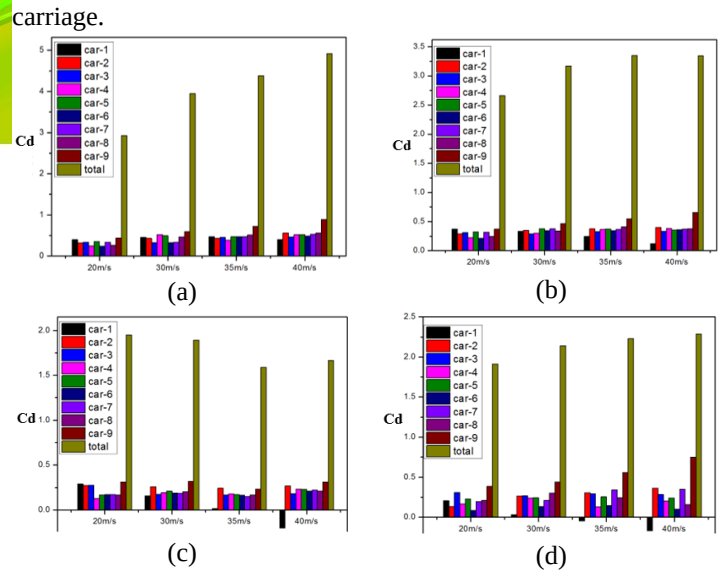

Figure 15. Comparison of aerodynamic drag of each carriage with different cross wind speeds: (a) Ground; (b) 3m-height embankment; (c) 6m-height embankment; (d) Viaduct.

When HSTs run in cross wind conditions, the lateral force of the leading car is an important variable that affects the running stability of the train. Figure 16 shows the lateral force coefficient of the leading car under different cross wind speeds. The lateral force of the leading car increases with the running speed for all the cases. However, the lateral force of the leading car is the smallest for the viaduct case. Part of the incoming cross wind flows beneath the bridge, which improve the ground effect in a certain extent.

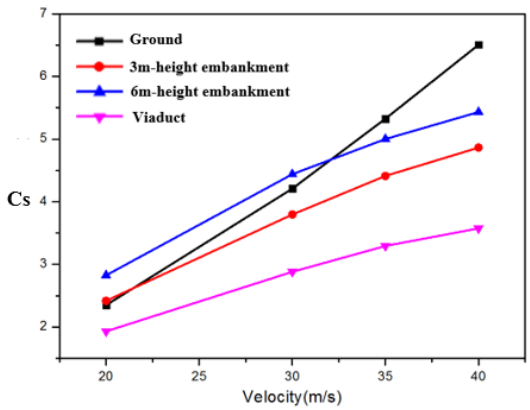

Figure 16. Lateral force coefficient of the leading car under different cross wind speeds

Aerodynamic lift could affect the interaction between the wheel and rail. Bigger lift would lead to smaller contact force, which could result in running instability. The aerodynamic lift of the trailing car is the most important one. Figure 17shows the aerodynamic lift of the trailing car for all subgrade structure cases. It could be observed that the lift for the ground case is the biggest under all cross wind speeds, while the lift for the 6m-height viaduct is the smallest. As the speed of cross wind increases, aerodynamic lift of the trailing car grows bigger and bigger.

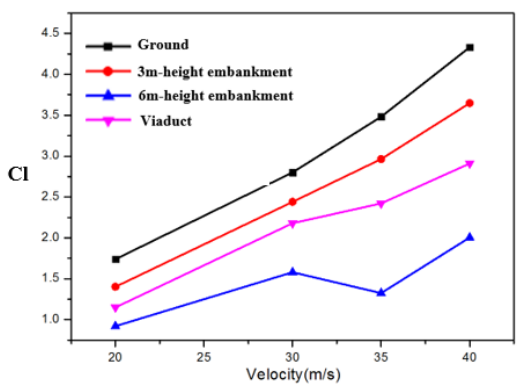

Figure 17. Aerodynamic lift force coefficient of the leading car under different cross wind speeds.

4 SHAPE DESCRIPTION METHODS

Four subgrade structures have been considered for the study of aerodynamic performance of HSTs in cross wind conditions. Comparison of the characteristics of the flow field and aerodynamic loads under different cross wind speeds and different subgrade structures has been performed. The main conclusions are as follows:

(1) Negative pressure exists on the leeward side of the train in cross wind conditions, and the area of negative pressure zone is bigger for the embankment cases than the ground case and the viaduct case.

(2) In cross wind conditions, the trailing vortex detaches from the shoulder of the trailing streamline. Meanwhile, smaller vortices exist around the bogies and windshields. For the embankment cases and viaduct case, vortex structures could be observed at the places with rough change of shapes.

(3) In the leeward side of the train, two vortex structures could be found, which generate from the trailing streamline, and grow bigger and stronger as they develop downstream.

(4) For the aerodynamic loads, the lateral force of each carriage and the aerodynamic lift of the trailing car increase with the cross wind speed. Meanwhile, the aerodynamic drag of the leading car decreases with the cross wind speed. Aerodynamic drag could act as thrust for the 6m-height embankment case and viaduct case when the cross wind speed reaches a certain value. Aerodynamic drag of the trailing car increases with the cross wind speed.

ACKNOWLEDGMENTS

This work was supported by Advanced Rail Transportation Special Plan in National Key Research and Development Project under 2016YFB1200601-B13. And Computing Facility for Computational Mechanics Institute of Mechanics, Chinese Academy of Sciences is gratefully acknowledged.

REFERENCES

[1] TIAN Hongqi. Train aerodynamics[M]. China Railway Publishing House, 2007: 304-305. (in Chinese)

[2] BAKER C J, JONES J, LOPEZ-CALLEJA F, et al. Measurements of the cross wind forces on trains[J]. Journal of Wind Engineering and Industrial Aerodynamics, 2004, 92(7): 547-563.

[3] BAKER C. The flow around high speed trains[J]. Journal of Wind Engineering and Industrial Aerodynamics, 2010, 98(6): 277-298.

[4] SUZUKI M, TANEMOTO K, MAEDA T. Aerodynamic characteristics of train/vehicles under cross winds[J]. Journal of Wind Engineering and Industrial Aerodynamics, 2003, 91(1): 209-218.

[5] DIEDRICHS B, SIMA M, ORELLANO A, et al. Crosswind stability of a high-speed train on a high embankment[J]. Proceedings of the Institution of Mechanical Engineers, Part F: Journal of Rail and Rapid Transit, 2007, 221(2): 205-225.

[6] BOCCIOLONE M, CHELI F, CORRADI R, et al. Crosswind action on rail vehicles: wind tunnel experimental analyses[J]. Journal of wind engineering and industrial aerodynamics, 2008, 96(5): 584-610.

[7] XI Yanhong, MAO Jun, GAO Liang, et al. Research on the limited safe speed of a high-speed train under cross wind[J]. Journal of the China Railway Society, 2012, 34(6): 8-14. (in Chinese)

[8] LI Tian, ZHANG Jiye, ZHANG Weihua. Dynamic performance of high-speed train passing windbreak in crosswind[J]. Journal of the China Railway Society, 2012, 34(7): 30-35. (in Chinese)

[9] ZHANG Liang, ZHANG Jiye, LI Tian, et al. Unsteady Aerodynamic Characteristics and Safety of High-speed Trains under Crosswinds[J]. Journal of Mechanical Engineering, 2016, 52(6): 124-135. (in Chinese)

[10] ZHANG Liang, ZHANG Jiye, LI Tian, et al. Research on Unsteady Aerodynamic Characteristics of Pantographs in Different Positions of High-speed Trains[J]. Journal of Mechanical Engineering, 2017, 53(12): 147-155. (in Chinese)

[11] MIAO Bingrong, TAN Shifa, WU Pingbo, et al. Research of Typical Fatigue Load Spectrum Simulation of Carbody Structure Based on Non-stationary Aerodynamic Load[J]. Journal of Mechanical Engineering, 2017, 53(10): 100-107. (in Chinese)

[12] HE Xuhui, ZOU Yunfeng, DU Fengyu. Mechanism analysis of wind barrier's effects on aerodynamic characteristics of a train on viaduct[J]. Journal of Vibration and Shock, 2015, 3, 66-71. (in Chinese)

[13] LUO Jianbin, HU Yuanyuan, YANG Jianheng, et al. Effect of Embankment Inclining Angle on Aerodynamic Characteristics of High Speed Train Under Crosswinds[J]. Chinese Journal of Computational Physics, 2013, 5, 675-682. (in Chinese)

[14] DC Wilcox., Turbulence Modeling for CFD, 2nd ed. La Caflada, CA: DCW Industries, Inc., 1998.

[15] GUO D, SHANG K, ZHANG Y, et al. Influences of affiliated components and train length on the train wind[J]. Acta Mechanica Sinica, 2016, 32(2): 191-205.